

**John D. Wright**  
Project Leader,  
Fluid Flow Group,  
e-mail: john.wright@nist.gov Mem. ASME

**Michael R. Moldover**  
Group Leader,  
Fluid Science Group

**Aaron N. Johnson**  
Fluid Flow Group

Process Measurements Division,  
Chemical Science and Technology Laboratory,  
National Institute of Standards and Technology,  
100 Bureau Drive,  
Gaithersburg, MD 20877

**Akisato Mizuno**  
Professor,  
Department of Mechanical Engineering,  
Kogakuin University,  
Nakano-Machi 2665,  
Hachioji-shi, Tokyo 192-0015, Japan

# Volumetric Gas Flow Standard With Uncertainty of 0.02% to 0.05%

*A new pressure, volume, temperature, and time (PVTt) primary gas flow standard for calibrating flowmeters has an expanded uncertainty ( $k=2$ ) of between 0.02% and 0.05%. The standard diverts a steady flow into a collection tank of known volume during a measured time interval. The standard spans the flow range of 1 slm<sup>1</sup> to 2000 slm using two collection tanks (34 L and 677 L) and two flow diversion systems. We describe the novel features of the standard and analyze its uncertainty. The thermostated collection tank allows determination of the average gas temperature to 7 mK (0.0023%) within an equilibration time of 20 min. We developed a mass cancellation procedure that reduced the uncertainty contributions from the inventory volume to 0.017% at the highest flow rate. Flows were independently measured throughout the overlapping flow range of the two systems and they agreed within 0.015%. The larger collection system was evaluated at high flows by comparing single and double diversions; the maximum difference was 0.0075%. [DOI: 10.1115/1.1624428]*

## Introduction

Accurate gas flow measurements are needed for quality, economy, and safety in the chemical process, manufacturing, and medical industries. Manufacturers of electronic components participating in a NIST organized workshop on mass flow controllers asked for primary flow standards with uncertainty of 0.025% to meet the needs of their industry, [1]. The most commonly used primary gas flow standards (piston provers and bell provers) have uncertainty of about 0.2%, [2]. Meanwhile, several generic flowmeter types show reproducibility of less than 0.05%. Therefore, the uncertainty of many gas flowmeters used in manufacturing processes is limited by the flow standards used to calibrate them. For these reasons, and to facilitate research into further improvements in gas flowmeters, NIST undertook a project to reduce the uncertainty of our primary gas flow standards by nearly an order of magnitude. Several novel features in the design and operation of the new PVTt system documented here were necessary to achieve our uncertainty goal.

PVTt systems have been used as primary gas flow standards for more than 30 years, [3–7]. The PVTt systems at NIST consist of a flow source, valves for diverting the flow, a collection tank, a vacuum pump, pressure and temperature sensors, and a critical flow venturi (CFV) (see Fig. 1).

The PVTt system measures flow using a volumetric timed-collection technique, whereby a steady flow is diverted into a nearly evacuated collection vessel of known volume for a measured time interval. The average gas temperature and pressure in the tank are measured before and after the filling process. These measurements are used to determine the density change and thereby the mass change in the collection volume. It is also necessary to consider the mass change in the inventory volume, a volume about 1/500th the size of the tank, bounded by the sonic line of the CFV and the two diverter valves (the gray region in

Fig. 1). By writing a mass balance for the control volume composed of the inventory and tank volumes (see the dashed line in Fig. 1), one can derive an equation for the average mass flow during the collection time:

$$\dot{m} = \frac{\Delta m_T + \Delta m_I}{\Delta t} = \frac{V_T(\rho_T^f - \rho_T^i) + V_I(\rho_I^f - \rho_I^i)}{t^f - t^i}, \quad (1)$$

where  $V_T$  and  $V_I$  are the tank and inventory volumes,  $\rho$  is the gas density determined via a real gas equation of state,  $t$  is time, and the superscripts  $i$  and  $f$  indicate initial and final values.

## Features of the New PVTt Standard

In order to achieve the uncertainty goal of 0.05% or better, we reviewed previous PVTt flow standards. We concluded that the new flow standard required (1) improved measurement of the average temperature of the collected gas and (2) reduced uncertainty of the mass change in the inventory volume. We met these requirements by designing a novel, well-thermostated collection tank and by adopting an inventory mass-cancellation procedure. These innovations are fully described in the following sections. Then, we describe the remaining important contributors

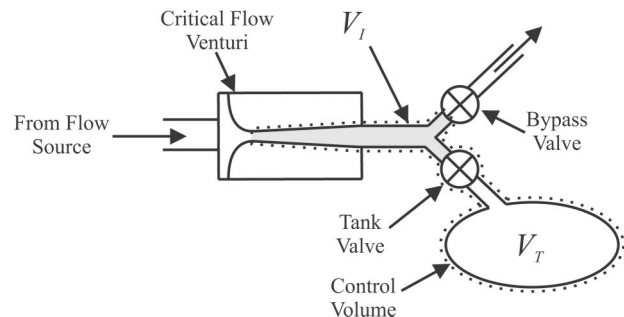
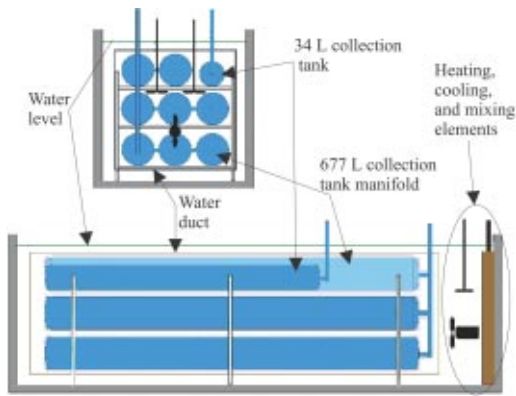


Fig. 1 Arrangement of equipment in the PVTt system

Contributed by the Fluids Engineering Division for publication in the JOURNAL OF FLUIDS ENGINEERING. Manuscript received by the Fluids Engineering Division Nov. 15, 2002; revised manuscript received June 4, 2003. Associate Editor: S. Cecio.

<sup>1</sup>slm=standard liters per minute, reference conditions are 293.15 K and 101.325 kPa.



**Fig. 2 Schematic diagram of the PVTt collection tanks, water bath, duct, and temperature control elements**

to the uncertainty of the new flow standard, namely, the determination of the tank volume and the determination of the density of the collected gas.

**Average Temperature of the Collected Gas.** One of the most important sources of uncertainty in a PVTt flow standard is the measurement of the average temperature of the gas in the collection tank, particularly after filling. The evacuation and filling processes lead to cooling and heating of the gas within the volume due to flow work and kinetic energy phenomena, [8]. The magnitude of the effect depends on the flow, however, the temperature rise in an adiabatic tank can be 10 K or more. Hence, immediately after filling and evacuation, significant thermal gradients exist within the collected gas. For a large tank, the equilibration time for the gas temperature can be many hours. If the exterior of the tank has non-isothermal or time varying temperature conditions, stratification and nonuniform gas temperatures will persist even after many hours.

In this flow standard, we avoided long equilibration times and the difficult problem of measuring the average temperature of a nonuniform gas by designing the collection tanks for rapid equilibration of the collected gas and by immersing the tanks in a well-mixed, thermostatted, water bath (see Fig. 2). Because the equilibration of the 677 L tank is slower, we consider it here. The 677 L tank is composed of eight 2.5 m long, stainless steel cylinders connected in parallel by a manifold. Each cylinder has a wall thickness of  $l=0.6$  cm and an internal radius of  $a=10$  cm. Because all of the collected gas is within 10 cm of a nearly isothermal cylinder, the gas temperature quickly equilibrates with that of the bath. After the collected gas equilibrates with the bath, the gas temperature is determined by comparatively simple measurements of the temperature of the recirculating water. In the following sections we describe the bath and the equilibration of the collected gas.

**The Water Bath.** The water bath is a rectangular trough 3.3 m long, 1 m wide, and 1 m high. Metal frames immersed in the bath support all the cylinders and a long duct formed by four polycarbonate sheets. The duct surrounds the top, bottom, and sides of the cylinders; however, both ends of the duct are unobstructed. At the upstream end of the bath, the water is vigorously stirred and its temperature is controlled near the temperature of the room (296.5 K) using controlled electrical heaters and tubing cooled by externally refrigerated, circulated water. A propeller pushes the stirred water through the duct along the cylinders. When the flowing water reaches the downstream (unstirred) end of the trough, it flows to the outsides of the duct and returns to the stirred volume through the unobstructed, 10 cm thick, water-filled spaces between the duct and the sides, the top, and the bottom of the rectangular tank.

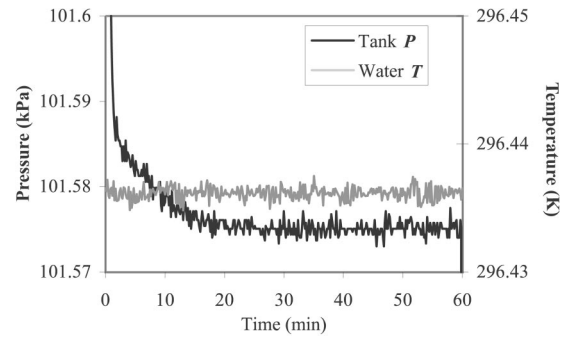


**Fig. 3 The collection tank pressure and the water bath temperature immediately following a tank filling, 25 slm in the 34 L tank**

The uniformity and stability of the water temperature was studied using 14 thermistors. The thermistors were bundled together and zeroed at one location in the water bath. Then, they were distributed throughout the water bath. Data recorded at 5 s intervals from these 14 thermistors over a typical 20 min long equilibration interval is generally within  $\pm 1$  mK of their mean and the standard deviation of the data from their mean is only 0.4 mK. The largest temperature transients occur where the mixed water enters the duct, indicating incomplete mixing. The tank walls attenuate these thermal transients before reaching the collected gas. Thus, after equilibration, the nonuniformity of the water bath and the fluctuations of the average gas temperature are less than  $\pm 1$  mK, which is equivalent to  $3 \times 10^{-6} T$ .

**Equilibration of the Collected Gas.** For design purposes, we estimated the time constant ( $\tau_g$ ) that characterizes the equilibration of the gas within the collection tank after the filling process. The estimate considers heat conduction in an infinitely long, isotropic, “solid” cylinder of radius  $a$ , [9]. For the slowest, radially symmetric heat mode,  $\tau_g = (a/2.405)^2/D_T$ , where  $D_T$  is the thermal diffusivity of the gas. This estimate gives  $\tau_g = 80$  s for nitrogen in the 677 L tank. This estimate for  $\tau_g$  is too large insofar as it neglects convection, conduction through the ends of the tanks, and the faster thermal modes, all of which hasten equilibration. The time constants for heat to flow from the gas through the tank walls and the time constant for a hot or cold spot within a wall to decay have been calculated and found to be less than a second. Therefore, we expect the collected gas to equilibrate with a time constant of less than 80 s.

The equilibration of the collected gas was observed experimentally by using the tank as a constant-volume gas thermometer. After the tank valve was closed, the pressure of the collected gas was monitored, as shown in Fig. 3. Our analysis of data such as those in Fig. 3 leads to the experimental values  $\tau_g$  of less than 60 s for both the 677 L and 34 L tanks, in reasonable agreement with the estimates. The measured time constant and Fig. 3 show that a wait of 20 min guarantees that the collected gas is in equilibrium with the bath, within the resolution of the measurements.

The manifold linking the eight cylindrical shells is completely immersed in the water bath. Thus, the gas in the manifold quickly equilibrates to the bath temperature as well. However, each collection system has small, unthermostatted, gas-filled volumes in the tubes that lead from the collection tanks to the diverter valves, the pressure transducers, etc. A temperature uncertainty from this source was calculated from the room temperature variations and the size of the volume outside the bath and it is, at most,  $4 \times 10^{-6} T$ . The combined uncertainty of the average gas temperature is 7 mK, and the largest contributor is, by far, the drift in the sensors between periodic calibrations. The relative standard uncertainty of the density of nitrogen gas in the full collection tank is

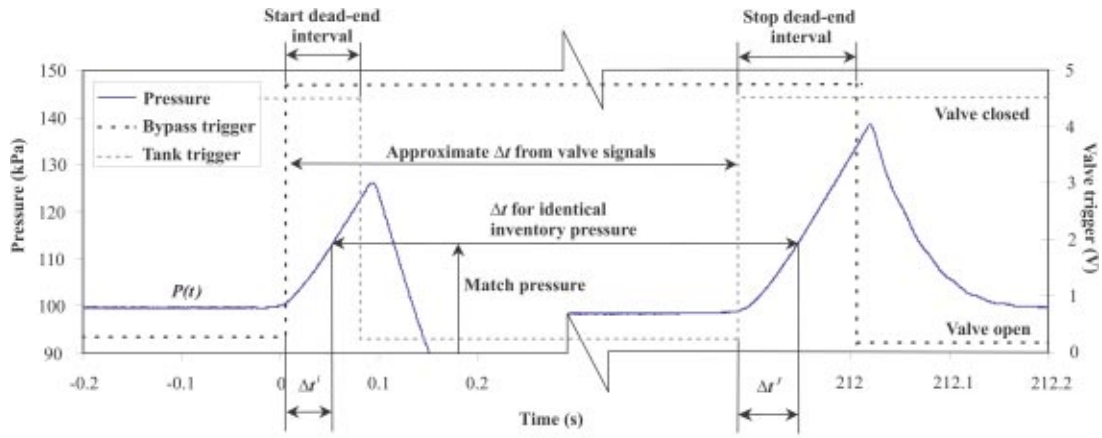


Fig. 4 Data from the pressure sensor in the inventory volume during a PVTt flow measurement, showing the transients that occur during the dead-end intervals

$68 \times 10^{-6}$ , and the largest contributor is the pressure measurement due to sensor calibration drift over time, [7] (see below).

### Mass Cancellation in the Inventory Volume

Figure 4 illustrates the changes in pressure within the inventory volume during the course of a single PVTt flow measurement. Initially, flow moves through the open bypass valve to the room while the collection tank is evacuated (tank valve closed) and the inventory pressure is nominally 100 kPa. When flow is diverted into the tank, there is a short period ( $<100$  ms) during which both the bypass and tank valves are closed to ensure clear accountability of the flow during diversion (the start dead-end time interval). During the dead-end time, steady-state flow continues to pass through the critical flow venturi (since the critical pressure ratio is maintained) and mass accumulates in the inventory volume. Hence a rapid rise in pressure and temperature (not shown) results. Once the valve to the evacuated tank opens, the inventory pressure drops to low values. The tank valve is left open until the tank fills to the initial inventory pressure (approximately 100 kPa) and then the flow is diverted back through the bypass valve, causing the stop dead-end time interval. Trigger voltages generated from the bypass and tank valve closed positions give approximate collection times. We will explain other elements of Fig. 4 later in this paper.

The start and stop times can be chosen at any point during the dead-end time intervals as long as the inventory conditions are measured coincidentally. Why is this true? Implicit in the PVTt mass balance (Eq. (1)) are two requirements: (1) the measurement of  $\rho_i^i$  and  $\rho_f^f$  (the initial and final densities) must be coincident with the measurement of  $t_i$  and  $t_f$  (the start and stop times) and (2) the only source or sink of mass to the control volume is the critical flow venturi. The second condition is met for the entire time that the bypass valve is fully closed, including the start and stop dead-end times. It is not necessary to determine  $m_T^i$  and  $m_T^f$  (the initial and final mass in the collection tank) coincidentally with  $t_i$  and  $t_f$  because  $m_T^i$  and  $m_T^f$  do not change while the tank valve is closed. Indeed, it is advantageous to measure  $m_T^i$  and  $m_T^f$  when the tank conditions have reached equilibrium.

It is difficult to determine either  $m_f^f$  or  $m_i^i$  within the inventory volume accurately (especially at high flows) because both the pressure and temperature in the inventory volume rise rapidly as the flow through the critical venturi accumulates in the inventory volume (see Fig. 5). However, it is possible to select  $m_T^i$  and  $m_T^f$  such that the difference  $m_f^f - m_i^i$  is nearly zero. We call our strategy for arranging this “mass cancellation.” Our strategy for dealing with the inventory mass change has two elements. First, by

design, the inventory volume  $V_I$  is much smaller than the collection tank volume  $V_T$ . ( $V_T/V_I = 500$  and  $700$  for the 34 L and 677 L systems, respectively.) Thus, the uncertainty of mass flow is relatively insensitive to uncertainty in  $m_f^f$  and  $m_i^i$  because both are small compared with the total mass of collected gas. Second, we choose  $t^i$  late in the dead-end time and we chose  $t^f$  such that  $P(t^f) = P(t^i)$ . With these choices, the initial and final inventory densities are essentially equal. In fact, we will assume that  $\Delta m_I$  is zero and consider the quantity only in terms of flow measurement uncertainty, not as part of the flow calculation.

In the remainder of this section, we describe conditions within the inventory volume during the dead-end times using both a model and measurements. The measurements show that  $T(t)$  and  $P(t)$  are nearly the same during the start and stop dead-end times. Finally, we show that  $\Delta m_I$  is insensitive to the exact choice of  $t^i$ , provided that the condition  $P(t^i) = P(t^f)$  is applied during the latter portion of the dead-end interval.

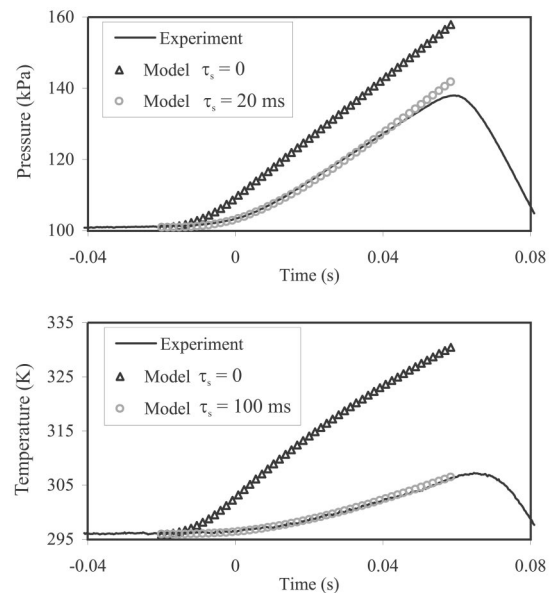


Fig. 5 Experimentally measured data (25 slm, 34 L collection system) and predictions for zero and nonzero sensor time constants. The predictions demonstrate that neglect of the sensors' response times would cause significant error in the measurement of inventory conditions.

**Conditions Within the Inventory Volume.** Figure 5 displays the time dependent temperature  $T(t)$  and pressure  $P(t)$  in the inventory volume during the dead-end interval of the smaller collection system at a typical collection rate ( $\dot{m}=25$  slm; collection time=82 s). The triangles in Fig. 5 were calculated from the lumped-parameter, thermodynamic model developed by Wright and Johnson [8], in this case for perfectly fast pressure and temperature sensors ( $\tau_s=0$ ). The model assumes a constant mass flow  $\dot{m}$  at the entrance to the inventory volume. The model neglects heat transport from the gas to the surrounding structure and non-uniform conditions, such as the jet entering the volume from the CFV outlet. For Fig. 5,  $T(t)$  and  $P(t)$  were calculated on the assumption that the diverter valve reduced the flow linearly (in time) to zero during the interval  $-0.02\text{ s}<t<0$ . Experimentally measured values of  $T(t)$  and  $P(t)$  recorded at 3000 Hz (smooth curves) are also shown in Fig. 5. Most of the differences between the measured curve and the calculated triangles ( $\tau_s=0$ ) result from the time constants of the sensors used to measure  $T(t)$  and  $P(t)$ . This is demonstrated by the agreement between the experimental curve and the model results when time constants are incorporated (circles).

In Fig. 5, the calculated curves do not display features that mark either the onset or the completion of the diverter valve closing. Thus, even  $T(t)$  and  $P(t)$  data from perfect sensors cannot be used to detect these events. For this reason,  $t^i$  and  $t^f$  were chosen such that they were clearly within the dead-end time intervals. We relied on the pressure sensor to choose  $t^i$  because the pressure responds more quickly than the temperature sensor and also because the pressure sensor responds to the average conditions throughout the inventory volume. In contrast, the temperature sensor responds primarily to the conditions at only one location. We choose  $t^i$  near the end of the dead-end time, where the  $P(t)$  measurements have nearly the same slope as the  $\tau_s=0$  model. In this regime, the dependence of  $P(t)$  on precisely how the valve closed has decayed. Therefore, we expect that  $P(t)$  will be the same during the start and the stop dead-end times, improving the mass cancellation as well as the correlation of initial and final inventory density uncertainties.

**Near Symmetry of Start and Stop Behavior of  $P(t)$ .** Figure 6 shows records of  $T(t)$  and  $P(t)$  taken during the dead-end time intervals at the start and stop of a single flow measurement. The data were recorded at 3000 Hz for 500 ms and the plots were displaced along the horizontal axis until they nearly overlapped. The pressure and the temperature at the beginning of the start dead-end time were slightly lower than those at the stop dead-end time (the “trigger pressure difference”); however, the two records match closely during the dead-end time. This implies that the time-dependent densities  $\rho(t)$  also nearly match.

At both diversions shown in Fig. 6, valve trigger signals were gathered along with the temperature and pressure measurements using a commercially manufactured data acquisition card (see Fig. 4). The trigger signals originate from an LED/photodiode pair and a flag on the valve actuator positioned so that the circuit output rises to a positive voltage when the valve is closed. These valve signals are used to trigger timers that give the approximate collection time.

As represented in Fig. 4, the inventory record is post-processed to obtain both the initial and final measurements of pressure and temperature in the inventory volume as well as the final collection time. An arbitrary “match pressure,”  $P(t^i)$ , that was measured late within the start dead-end time is selected. The same value of the pressure is found in the stop data series and the time differences between the match pressure measurements and the start and stop trigger signals are determined from the data record ( $\Delta t^i$  and  $\Delta t^f$ ). These time corrections are used to correct the approximate times from the trigger signals and calculate the time interval between matching inventory pressures. As shown in Fig. 6, the tem-

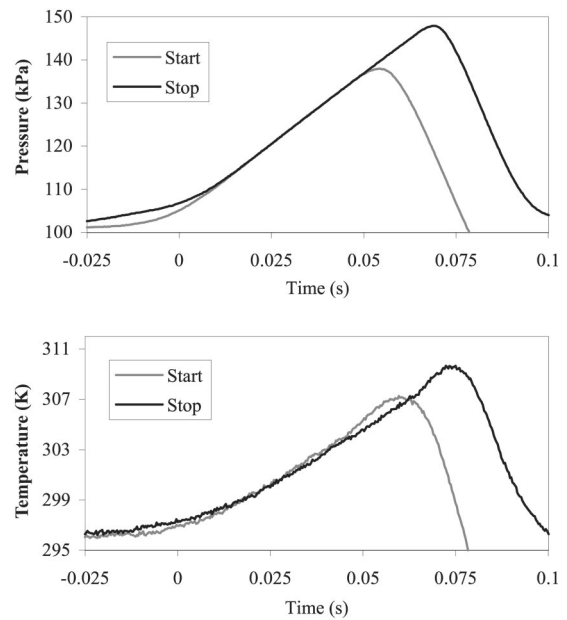


**Fig. 6 Superimposed inventory data traces for a start diversion and a stop diversion in the 34 L tank at 25 slm demonstrating “symmetric” diverter valve behavior. The start dead-end time was approximately 50 ms; the stop dead-end time was approximately 15 ms longer.**

peratures are also nearly matched; thus, the initial and final inventory densities nearly match and inventory mass cancellation occurs.

**Uncertainty of  $\Delta m_I$ .** Imperfections of the mass cancellation procedure contribute to the uncertainty of  $\Delta m_I$ . The most significant of these uncertainty components (due to sensor time constants) are correlated between the start and stop diversions. Other correlated inventory volume uncertainties include the pressure and temperature sensor calibrations and the differences between sensed and stagnation values of pressure and temperature. The uncertainty of the mass change within the inventory volume caused by the *correlated* pressure and temperature uncertainties can be expressed as

$$u(\Delta m_I) = \frac{V_I M}{ZR} \left[ \left( \frac{1}{T_I^i} u(P_I^f) - \frac{1}{T_I^f} u(P_I^i) \right)^2 + \left( \frac{P_I^f}{(T_I^f)^2} u(T_I^f) - \frac{P_I^i}{(T_I^i)^2} u(T_I^i) \right)^2 \right]^{1/2} \quad (2)$$

where in this equation,  $u(P_I)$ ,  $u(T_I)$ , and  $u(\Delta m_I)$  are the uncertainties of the inventory pressure, inventory temperature, and inventory mass change during the collection, respectively. Note that if the uncertainties and the initial and final conditions are equal (i.e.,  $u(T_I^i) = u(T_I^f)$ ,  $u(P_I^i) = u(P_I^f)$ ,  $T_I^i = T_I^f$ , and  $P_I^i = P_I^f$ ), then the terms within parentheses cancel, and the flow uncertainty related to the inventory volume is zero. Equation (2) demonstrates the benefit of matching the initial and final inventory conditions to optimize the cancellation of correlated uncertainties.

Not all of the measurement uncertainties of the inventory volume are correlated. Inconsistencies in the pressure and temperature fields may originate from a change in the inventory wall temperature or from differences in the flow paths between the start and stop diversions. In our uncertainty analysis, we assumed that the spatial inconsistencies are uncorrelated and that their magnitude is proportional to the mass flow. Hence, the inventory uncertainties are negligible at the lowest flows for each system, but account for about half the mass flow uncertainty under high flow

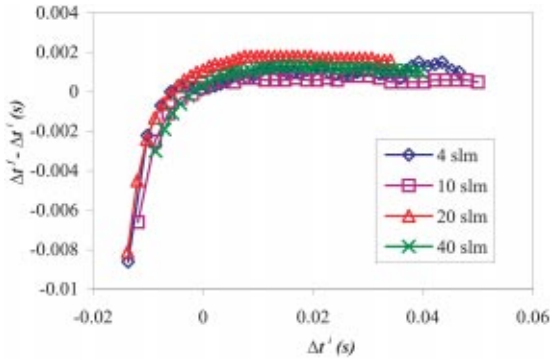


**Fig. 7 The time correction for the 34 L tank versus the time relative to the trigger signal indicating bypass valve closure**

conditions. Maximum values for the uncorrelated inventory uncertainties of 3 kPa and 9 K were assumed and their magnitude was verified by the flow comparison and double-diversion experiments described later.

**Insensitivity of  $\Delta m_I$  to the Match Pressure.** For a perfectly symmetric diverter system (identical tank and bypass valves and identical “start-diversion” and “stop-diversion” pressures), and with a perfectly fast pressure sensor ( $\tau_s = 0$ ), the correction time ( $\Delta t^f - \Delta t^i$ ) would be a constant for any point in the dead-end time interval. For the real system, the best correction times are calculated during the latter portion of the dead-end time, after the effects of trigger pressure differences and the flow differences during valve closure have decayed from the pressure sensor measurements.

Figure 7 shows the total correction time ( $\Delta t^f - \Delta t^i$ ) versus the initial time correction ( $\Delta t^i$ ) for several flows in the 34 L system. For values of  $\Delta t^i$  less than zero (i.e., the bypass valve is in the process of closing), the time corrections are as large as 10 ms. Later in the dead end time ( $\Delta t^i > 10$  ms) the time corrections are near zero and constant to within 0.5 ms (for a given flow). The time corrections are nearly constant after the differences in the mass flow between the two valve closures and the trigger pressure differences have decayed from the  $\tau_s = 20$  ms pressure sensor. The experimental results given in Fig. 7 and the Wright-Johnson model show that matching the conditions late in the dead-end interval (i.e., at times  $> 2\tau_s$ ) result in nearly constant correction times, while low match pressures (early in the dead-end time) give much larger corrections.

Figure 7 also illustrates the concept that uncertainties related to the inventory volume can be treated not only as mass measurement uncertainties, but as time measurement uncertainties as well. One can consider the uncertainty in the measurement of time between conditions of perfect mass cancellation, or one can consider the uncertainty in the measurement of inventory mass differences between the start and stop times. Both perspectives offer insight and verification of the uncertainties of the inventory volume and flow diversion process.

## Measurement of the Tank and Inventory Volumes

**Gas Gravimetric Method.** The volume of the 677 L tank was determined by a gas gravimetric method. In this method, the mass of an aluminum high pressure cylinder was measured before and after discharging its gas into the evacuated collection tank. The change in mass of the high pressure cylinder and the change in density of the gas in the collection tank were used to calculate the collection tank volume,  $V_m$ . Nominally,

$$V_m = \frac{m_c^i - m_c^f}{\rho_T^f - \rho_T^i} - V_e, \quad (3)$$

where the  $m_c$  indicates the mass of the high pressure cylinder and  $V_e$  is the small volume within the tubing and the valve body that temporarily connected the collection tank to the high pressure weighing cylinder. The extra volume is calculated from dimensional measurements or measured by liquid volume transfer methods. The density of the gas in the collection tank ( $\rho_T^f$  and  $\rho_T^i$ ) was measured with a relative standard uncertainty of  $68 \times 10^{-6}$ , as discussed below.

In practice, a more complex formula than Eq. (3) was used to account for a small amount of gas that enters the control volume from the room when the cylinder is disconnected from the collection tank because the final tank pressure was less than atmospheric. For the volume determinations performed for the 677 L tank, the effect amounts to only  $5 \times 10^{-6} V$ .

Independent volume determinations were conducted with both nitrogen and argon gas. In all cases, high purity gas was used (99.999 % mol fraction) and care was taken to evacuate and purge the system. When nitrogen was used, the aluminum cylinder weighed approximately 4200 g when filled at 12.5 MPa, and approximately 3800 g after it was emptied to 55 kPa. When argon was used, the initial and final masses were 4440 g and 3820 g, respectively. The standard deviation of the six volume measurements (4 with nitrogen, 2 with argon) was  $16 \times 10^{-6} V$ .

The initial and final masses of the gas cylinder were measured using a substitution process with reference masses and a mass comparator enclosed in a wind screening box. The comparator has a full scale of 10 kg and resolution of 1 mg. The cylinder and a set of reference masses of nearly the same weight were alternated on the scale five times. The zero corrected scale readings were then calibrated to the reference masses and buoyancy corrected via the following formula:

$$m_c = \frac{S_c}{S_r} m_r \left( 1 - \frac{\rho_a}{\rho_r} \right) + \rho_a V_o, \quad (4)$$

where  $S$  represents the scale reading, the subscripts  $r$  and  $c$  indicate the reference masses and the cylinder respectively,  $\rho_a$  is the ambient air density where the measurements were conducted, and  $V_o$  is the external volume of the high pressure cylinder and its valve and fittings. The density of the ambient air was calculated from the barometric pressure, the temperature and humidity inside the wind screen, and an air density formula that includes humidity, [10]. The cylinder mass was measured with a relative standard uncertainty of  $1 \times 10^{-6}$ .

The external volume of the high pressure cylinder appears in Eq. (4) due to air buoyancy corrections. The external volume of the cylinder was measured by Archimedes principle, i.e., by measuring the change in apparent mass of the object in air and in distilled water. The thermal expansion corrections to the external volume were less than 0.5 mL ( $100 \times 10^{-6} V_o$ ) and were not significant since the external volume has a small sensitivity coefficient in the collection tank volume determination process. The expansion of the external cylinder volume as a function of its internal pressure was not negligible. The Archimedes principle measurements showed a volume increase from 4697.5 mL to 4709 mL between the 100 kPa and 12.5 MPa pressures. This change agreed well with predictions based on material properties, and the appropriate experimental values for external volume were used in the cylinder mass calculations (Eq. (4)), depending on whether the cylinder was empty or full. If this issue were neglected, it would lead to errors in the mass change measurements of about  $35 \times 10^{-6} \Delta m_c$ .

In summary, the gravimetric determinations of the 677 L collection tank volume made with nitrogen and with argon agreed with each other; the mean of the six measurements had a standard deviation of  $16 \times 10^{-6} V_T$ . Because the volume was measured at essentially the same pressure and temperature at which it is used for flow measurements, changes in  $V_T$  due to pressure dilation and

thermal expansion are negligible. The gas density of the full collection tank contributed 92 % of the uncertainty of  $V_T$ . This is discussed below.

**Volume Expansion Method.** The 34 L collection tank volume, the inventory volume for the large collection tank, and the small inventory volume were all determined via a volume expansion method. In this method, a known volume is pressurized, the unknown volume is evacuated, a valve is opened between the two volumes, and the resulting density changes within the two volumes are used to calculate the unknown volume. Applying conservation of mass to the system of the two tanks yields

$$V_2 = \frac{(\rho_1^f - \rho_1^i)V_1}{(\rho_2^i - \rho_2^f)} - V_e, \quad (5)$$

where the subscripts 1 and 2 refer to the known and unknown volumes, respectively. As before, the density values are based on pressure and temperature measurements of the gas within the volumes and gas purity issues must be considered. Note that in many cases the final densities can be considered the same in both volumes 1 and 2, but for the determination of the 34 L tank volume, elevation differences between the two tanks required a head correction to the pressure measurements and therefore the two densities were not strictly equal. The difference in elevation resulted in a relative difference in gas density of  $20 \times 10^{-6}$  even though the two tanks were connected. The relative standard uncertainty of the 34 L tank volume was  $116 \times 10^{-6}$ , and the largest contributors were the known 677 L volume and the density change in the 34 L tank (traceable to the measurement of pressure change).

### Density in the Collection Tank

The density of the nitrogen (or argon) in the collection tank was determined from measurements of the gas pressure, temperature of the water bath, and the equation of state, as correlated in the NIST database Refprop 23, [11]. Of these, the pressure measurement contributed most to the uncertainty. The pressure was measured with a 200 kPa full-scale absolute pressure transducer. For the 100 kPa and 296 K conditions present in the full collection tank, the pressure measurement uncertainty is  $64 \times 10^{-6} P$  and the temperature uncertainty is  $17 \times 10^{-6} T$ . For both pressure and temperature measurements, the largest source of uncertainty is sensor drift between periodic calibrations. The equation of state contributes a relative uncertainty of  $10 \times 10^{-6}$  to the density determinations and more detail about all of these uncertainty sources can be found in Ref. [7].

### Mass Flow Uncertainty

The uncertainty of a mass flow measurement made with the PVTt standard was calculated following the propagation of uncertainties techniques described in the ISO Guide to the Expression of Uncertainty in Measurement, [12]. The uncertainty of each of the inputs to a flow measurement is determined, weighted by its sensitivity, and combined with the other uncertainty components

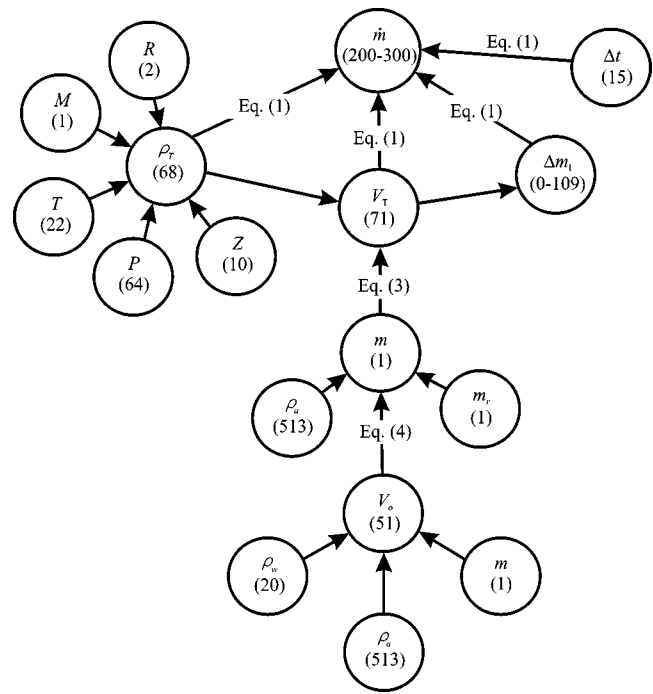


**Fig. 8 The chain of measurements and equations used for the PVTt flow standard. The subcomponents are labeled with their relative standard uncertainty  $\times 10^6$  ( $k=1$ ) for the 677 L system. The mass flow uncertainty is a  $k=2$  or approximately 95% confidence value.**

by root-sum-square (RSS) to arrive at a combined uncertainty. Figure 8 schematically lists the components that have been considered in the uncertainty analysis and their relationship to the mass flow measurement. The uncertainties of the components have been quantified in detail in a prior publication, [7].

The uncertainty for flows between 20 slm and 2000 slm of nitrogen in the 677 L tank is given in Table 1 and in Fig. 8. The standard uncertainty of each subcomponent is given in both relative ( $\times 10^6$ ) and dimensional forms. The units of the dimensional values are given. The relative contribution of each subcomponent to the combined uncertainty is listed in the fourth column. This contribution is the %age of the squared individual component relative to the sum of the squares of all subcomponents. The uncertainty from the inventory volume, the combined uncertainty, the expanded uncertainty, and the uncertainty contributions are given as a range covering the minimum to maximum flow.

At the highest flow, uncertainty contributions are principally divided between the tank volume, the final gas density, and the inventory uncertainty. The relative expanded uncertainty falls to  $200 \times 10^{-6}$  for the smallest flows as the uncertainty contributions of the inventory volume become negligible. For an air flow mea-

**Table 1 Uncertainty of measuring nitrogen flows from 20 slm to 2000 slm with the 677 L standard**

Uncertainty Category Flow (677 L, N <sub>2</sub> )	Standard Uncertainty ( $k=1$ )		Contribution (%)
	Relative ( $\times 10^6$ )	Dimensional	
Tank volume	71	48.5 cm <sup>3</sup>	50 to 23
Tank initial density	10	$1.14 \times 10^{-8}$ g/cm <sup>3</sup>	1 to 0
Tank final density	68	$7.77 \times 10^{-8}$ g/cm <sup>3</sup>	45 to 21
Inventory mass change	0 to 109	(0 to 0.084) g	0 to 53
Collection time	15	0.287 ms	0 to 1
Std deviation of repeated meas.	20	0.001 g/s	4 to 2
<b>RSS (combined uncertainty)</b>	102 to 150		
<b>Expanded uncertainty (<math>k=2</math>)</b>	204 to 300		

**Table 2 Uncertainty of measuring nitrogen flows from 1 slm to 100 slm with the 34 L standard**

Uncertainty Category Flow (34 L, N <sub>2</sub> )	Standard Uncertainty ( $k=1$ )		Contribution (%)
	Relative ( $\times 10^6$ )	Dimensional	
Tank volume	116	4.0 cm <sup>3</sup>	72 to 28
Tank initial density	10	1.14E-08 g/cm <sup>3</sup>	1 to 0
Tank final density	68	7.77E-08 g/cm <sup>3</sup>	25 to 10
Inventory mass change	0 to 170	(0 to 0.007) g	0 to 61
Collection time	15	0.287 ms	0 to 0
Std deviation of repeated meas.	20	4.0E-05 g/s	2 to 1
<b>RSS (combined uncertainty)</b>	<b>137 to 219</b>		
<b>Expanded uncertainty (<math>k=2</math>)</b>	<b>274 to 438</b>		

surement, the relative expanded uncertainty of the 677 L system must be increased to approximately  $500 \times 10^{-6}$  over the entire flow range because the moisture content of the compressed air is not well controlled. Then, the largest uncertainty is the density of the air in the collection tank (80% contributor).

The standard uncertainty of the tank final density ( $68 \times 10^{-6} \rho_T$ ) is a large contributor to both the tank volume determination as well as the mass flow measurement. The most significant contributions to the density uncertainty are pressure (88%) and temperature (10%). The largest uncertainty contributions to the pressure and temperature measurements are calibration drift between calibrations (88% and 77%, respectively). Therefore sensors with more stable calibrations, particularly for pressure, would dramatically improve the uncertainty of mass flow measurements.

Table 2 presents the uncertainty of flow measurements from the 34 L system for flows between 1 slm and 100 slm. The relative expanded uncertainty varies between  $270 \times 10^{-6}$  and  $440 \times 10^{-6}$ . At high flows, the significant uncertainty sources are the tank volume, the tank final density, and the uncorrelated inventory uncertainties. For low flows, the major contributors are tank volume and final gas density. For air flow measurements, the 34 L system has a nearly constant relative expanded uncertainty over its entire flow range of approximately  $500 \times 10^{-6}$ . The largest contribution to this is the uncertainty of the density of the humid air in the collection tank.

## Experimental Validation of the Uncertainty Analysis

**Comparison of the 34 L and 677 L Flow Standards.** We conducted flow comparisons between the 34 L and the 677 L flow standards to test the mass cancellation strategy and the validity of the uncertainty analyses. To test the 34 L system, we conducted calibrations of critical flow venturis at identical flows spanning the range  $3 \text{ slm} < \dot{m} < 100 \text{ slm}$  (0.06 g/s to 2.3 g/s) in both the small and the large systems. The large system can be used as a reference for the small system because its inventory (and total) uncertainties are quite small in this flow range. The collections ranged from as short as 18 s to more than 4 hours.

Figure 9 shows the difference in the discharge coefficients of several critical flow venturis as measured by the 34 L and 677 L systems, plotted versus flow. The maximum disagreement between the two flow standards is less than  $150 \times 10^{-6} \dot{m}$  over the entire range tested. The throat diameters of the venturis used for the comparisons ranged between 0.3 mm and 1.7 mm. The comparisons were done with the same pressure and temperature sensors associated with the CFV during the testing on both flow standards in order to reduce some possible sources of discharge coefficient differences. Numerous collections were made for each tank at each flow to confirm stability of the conditions at the critical flow venturi.

How well should the two systems agree? The difference between the discharge coefficients measured by the two PVT systems should be less than the RSS of the uncertainties of the two standards, especially when one considers that the uncertainties due to pressure and temperature measurements are correlated be-

tween the two standards. For the lowest flows of the comparison range, the uncertainties originating from the inventory volume are quite small for both systems and the observed differences between them are dominated by tank volume uncertainties. From Fig. 9 it can be seen that the two systems differ by about  $100 \times 10^{-6} \dot{m}$  for flows less than 20 slm. The RSS of the two relative volume uncertainties from Tables 1 and 2 is  $137 \times 10^{-6}$  ( $k=1$ ).

At the higher flows of the comparison range, the uncertainties associated with the transient conditions in the inventory volume should be negligible in the 677 L system; however, they will increase with flow for the 34 L system. Because the collection times were 1/20th as long when using the smaller tank, any timing error (or, equivalently any imperfection of the mass cancellation technique) was 20 times more important for the smaller tank. Figure 9 suggests that the transient conditions cause a bias such that the 34 L flow standard reads too high as the flow is increased. The bias is approximately  $200 \times 10^{-6} \dot{m}$  at the largest flow compared. This bias is comparable to the  $170 \times 10^{-6}$  ( $k=1$ ) of relative uncertainty contributed by the inventory volume at the highest flows in the 34 L system according to our uncertainty analysis (see Table 2). Therefore, the bias observed in the comparison is consistent with the uncertainty analysis.

Figure 9 also examines the tank comparison results from the perspective of time measurement uncertainty rather than the mass. We interpreted the comparison results using the simplified model  $\dot{m} = m/t$ , where  $m$  is the mass collected and  $t$  is the collection time using the 34 L tank. If we assume that a constant bias  $\delta m$  is present in all of the mass measurements for all flows (for example, from an error in the volume of the 34 L tank) and that a constant bias  $\delta t$  is present in all the time measurements (for example from differing responses of the pressure sensor to closing the tank valve

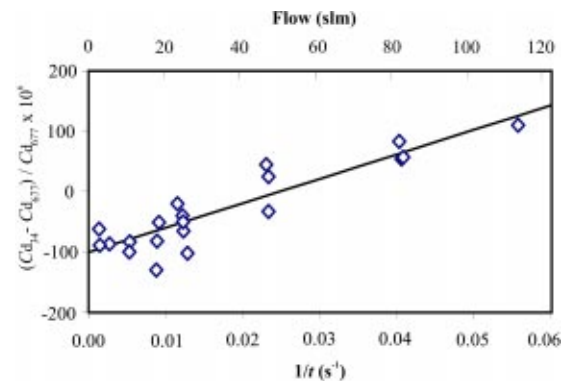


**Fig. 9 Relative difference in the discharge coefficient of critical flow venturis calibrated on both the 34 L ( $C_{d34}$ ) and 677 L ( $C_{d677}$ ) flow standards versus flow and the inverse of the collection time for the 34 L tank. Also plotted is a linear best fit of the data.**

and the bypass valve) we expect that the bias of the mass flow measurement will be a linear function of the inverse collection time, i.e.,

$$\frac{\delta \dot{m}}{\dot{m}} = \frac{\delta m}{m} - \frac{\delta t}{t} \quad (7)$$

The measurements in Fig. 9 are consistent with such a linear function. The slope implies a constant timing error of 4 ms. A timing error of this order is not surprising because the timing is based on a pressure sensor with a time constant of approximately 20 ms. The relative standard deviation of the flow measurements from the best fit line is  $24 \times 10^{-6}$ .

The intercept of the line in Fig. 9 could be used to “correct” the volume of the 34 L tank, thereby improving the agreement between the two systems at low flows. The slope of the line in Fig. 9 could be used to improve agreement at higher flows. If this were done, the comparison differences would be zero with a standard deviation of  $24 \times 10^{-6} \dot{m}$ . These corrections have not been made at the present time for four reasons. (1) The comparison results are consistent with the present uncertainty analysis. (2) We plan to improve the measurements of the pressure in the inventory volume; this may reduce the slope in the comparison data. (3) We plan to refine the volume expansion process used to determine the 34 L tank size; this may reduce the apparent volume difference. (4) By refraining from making a correction, we adhere to the definition of a primary standard for both collection systems because both have been calibrated with reference to SI units, not with reference to another flow standard.

During some of the comparison flows, we noticed that the pressure downstream of the critical flow venturi was significantly higher in the 34 L system than in the 677 L system (108 kPa versus 100 kPa) due to the smaller tube size and resultant higher pressure drop. For some of our venturis (with relatively short diffusers) this pressure difference caused slight changes in the upstream pressure (and the discharge coefficient), even at conditions well above the critical pressure ratio. Therefore, our assumption that for the same throat Reynolds number, the discharge coefficient of the venturi is independent of the downstream pressure may not be completely valid. We suspect that some of the differences observed between the tanks in Fig. 9 are due to the venturis (even though long diffusers were used).

In one series of experiments, the trigger pressure difference was intentionally varied over the range from  $-2$  kPa to 27 kPa at the constant flow of 82 slm in the 34 L system. The purpose of the test was to measure the dependence of the venturi discharge coefficient on the trigger pressure difference and hence to assess its influence on the inventory uncertainties. The tests showed a relative change of  $10 \times 10^{-6}$  in discharge coefficient for each 1 kPa change in the trigger pressure difference. Because the largest trigger pressure difference is less than 3 kPa in the present system, this effect is expected to contribute only  $30 \times 10^{-6}$  to the flow uncertainty. If further measurements confirm this, we must admit that the major contributor to the slope in Fig. 9 is unknown. Perhaps it is an inconsistency of the pressure and temperature fields between the start and stop diversions.

**Multiple Diversions in the 677 L Flow Standard.** To independently test the uncertainty analysis for the inventory volume of the 677 L collection system, we performed CFV calibrations at identical flows following two different protocols. In the first protocol, the inventory volume was dead-ended at the beginning and end of the collection interval, in the usual manner. In the second protocol, the collection interval was divided into two subintervals, i.e., each flow measurement had two start and stop diversions. If the mass cancellation procedure introduced a bias  $\Delta m_I$ , the second protocol would double this bias and allow assessment of its uncertainty contribution. The CFV discharge coefficients from the two protocols were compared to assess the magnitude of the uncertainties introduced by the inventory volume and the flow diver-

**Table 3 Differences in CFV discharge coefficients ( $C_d$ ) for two and one diversion in the 677 L flow standard**

Flow (slm)	$[C_d(2 \text{ Diversions}) - C_d]/C_d \times 10^6$
300	$53 \pm 25$
700	$-27 \pm 31$
1600	$75 \pm 122$

sion process. Three flows between 300 slm and 1600 slm were tested. The two protocols produced relative differences in discharge coefficient that were all less than  $75 \times 10^{-6}$  (see Table 3), which is within the relative standard uncertainty assumed in the analysis ( $109 \times 10^{-6}$  in Table 1).

## Conclusions

The design of a new gas flow standard composed of two PVTt collection tanks (34 L and 677 L) has been presented. The system is designed to calibrate critical flow venturis for flows from 1 slm to 2000 slm. The flow standard has several novel features. The collection tanks are immersed in a water bath that matches the nominal room temperature and is stable and uniform to better than 1 mK. The collection tanks are divided into sections of small enough diameter that the gas inside them achieves thermal equilibrium with the surrounding water bath in 20 min or less. This reduces the contribution of temperature to the flow measurement uncertainty to a very low level.

Uncertainties related to the inventory volume and the diversion of gas into the collection tank at the start and stop of a flow measurement have been studied in great detail. A thermodynamic model of the inventory volume during diversion was utilized to understand the importance of large pressure and temperature transients and of sensor time constants on the flow measurement uncertainty. The flow standard is operated to achieve “mass cancellation” in the inventory volume, thereby taking advantage of correlated sensor uncertainties to minimize uncertainty contributions from the inventory volume.

An uncertainty analysis for the mass flow measurements from the two systems has been presented. The analysis used the PVTt basis equation and followed the propagation of uncertainties method suggested by international standards. The uncertainty analysis shows that the 677 L system measures mass flow with a relative expanded uncertainty between  $200 \times 10^{-6}$  and  $300 \times 10^{-6}$  for a pure gas like nitrogen or argon, where the higher uncertainty applies to higher flows. For the 34 L tank and pure gases, the relative expanded uncertainties range from  $270 \times 10^{-6}$  to  $440 \times 10^{-6}$ . The uncertainties are larger for the 34 L tank because the tank volume uncertainty is greater and the ratio of collection tank volume to inventory volume is smaller for the small system. For pure gas measurements, the largest sources of uncertainty can be traced to pressure measurement ( $64 \times 10^{-6} P$ ) which is the major contributor to both gas density and tank volume uncertainties. For air flow measurements using gas from a compressor and drier, mass flow relative expanded uncertainties are about  $500 \times 10^{-6}$  for both standards and the major contribution is the uncertainty in the moisture content of the air.

Comparisons between the 34 L and 677 L standards from 3 slm to 100 slm show agreement within  $150 \times 10^{-6} \dot{m}$  or better. Experiments using single diversions (normal operation) and double diversions to the collection tank were used to validate the uncertainty estimates of the 677 L inventory volume and the differences between these two methods were less than  $75 \times 10^{-6} \dot{m}$ . The evaluation results along with comparisons to previously existing gas flow standards support the uncertainty statements for the new standards.

## Nomenclature

$a$	=	radius of gas collection tank
$C_d$	=	discharge coefficient for a critical flow venturi
$D_T$	=	thermal diffusivity
$k$	=	uncertainty coverage factor
$m$	=	mass
$M$	=	molecular weight
$P$	=	pressure
$R$	=	universal gas constant
$T$	=	temperature
$t$	=	time
$u(x)$	=	uncertainty of quantity $x$
$V$	=	volume
$Z$	=	compressibility
$\rho$	=	density
$\tau$	=	time constant

## Subscripts

$a$	=	ambient air
$c$	=	cylinder
$e$	=	extra
$g$	=	gas
$I$	=	inventory
$m$	=	gravimetric
$o$	=	external
$r$	=	reference
$s$	=	sensor
$T$	=	tank
$w$	=	water
1	=	known
2	=	unknown

## Superscripts

$i$	=	initial
$f$	=	final

## Acronyms

CFV	=	critical flow venturi
PVTt	=	pressure, volume, temperature, and time
RSS	=	root sum square

## References

- [1] Berg, R., Green, D., and Mattingly, G., 2000, *Semiconductor Measurement Technology: Workshop on Mass Flow Measurement and Control for the Semiconductor Industry*, NIST Special Publication 400-101, National Institute of Standards and Technology, Gaithersburg, MD, p. 17.
- [2] Wright, J., 2003, "What is the 'Best' Transfer Standard for Gas Flow?" *Proceedings of FLOMEKO*, Groningen, The Netherlands.
- [3] Olsen, L., and Baumgarten, G., 1971, "Gas Flow Measurement by Collection Time and Density in a Constant Volume," *Flow: Its Measurement and Control in Science and Industry*, The Instrumentation, Systems, and Automation Society, Research Triangle Park, NC, pp. 1287-1295.
- [4] Kegel, T., 1995, "Uncertainty Analysis of a Volumetric Primary Standard for Compressible Flow Measurement," *Proceedings of Flow Measurement 3rd International Symposium*, San Antonio, TX, Colorado Engineering Experiment Station, Nunn, Co.
- [5] Ishibashi, M., Takamoto, M., and Watanabe, N., 1985, "New System for the Pressurized Gas Flow Standard in Japan," *Proceedings of International Symposium on Fluid Flow Measurements*, American Gas Association.
- [6] Wright, J., 2001, "Laboratory Primary Standards in Flow Measurement," *Flow Measurement: Practical Guides for Measurement and Control*, 2nd Ed., D. W. Spitzer ed., The Instrumentation, Systems, and Automation Society, Research Triangle Park, NC, pp. 731-760.
- [7] Wright, J., Johnson, A., and Moldover, M., 2003, "Design and Uncertainty Analysis for a PVTt Gas Flow Standard," *J. Res. Natl. Inst. Stand. Technol.*, **108**, pp. 21-47.
- [8] Wright, J., and Johnson, A., 2000, "Uncertainty in Primary Gas Flow Standards Due to Flow Work Phenomena," *Proceedings of FLOMEKO*, Salvador, Brazil, Institute for Technological Research, Sao Paulo, Brazil.
- [9] Carslaw, H., and Jaeger, J., 1946, *Conduction of Heat in Solids*, 2nd Ed., Clarendon Press, Oxford, pp. 198-201.
- [10] Jaeger, J., and Davis, R., 1984, *A Primer for Mass Metrology*, NBS Special Publication 700-1, National Bureau of Standards, Gaithersburg, MD, p. 22.
- [11] Lemmon, E., McLinden, M., and Huber, M., 2002, *Refprop 23: Reference Fluid Thermodynamic and Transport Properties*, NIST Standard Reference Database 23, Version 7.0, 7/30/02, National Institute of Standards and Technology, Boulder, CO.
- [12] International Organization for Standardization, 1996, *Guide to the Expression of Uncertainty in Measurement*, Switzerland.